International Journal of Nanoelectronics and Materials
IJNeaM
ISSN 1985-5761 | E-ISSN 2232-1535

The turkevich method revisited: A comprehensive guide to molar ratio control in the synthesis of 15 nm gold nanoparticles for beginners

Anis Diyana Rosli[a], Nor Shahanim Mohamad Hadis[a]*, Zurita Zulkifli[b], Afaf Rozan Radzol[a], Rosfariza Radzali[a], Aida Zulia Zulhanip[a]

[a]*Electrical Engineering Studies, Universiti Teknologi MARA, Cawangan Pulau Pinang, Permatang Pauh Campus, 13500 Permatang Pauh, Pulau Pinang, Malaysia*
[b]*Faculty of Electrical Engineering, Universiti Teknologi MARA, 40450 Shah Alam, Selangor Darul Ehsan, Malaysia*
**Corresponding author. E-mail: norsh713@uitm.edu.my*

Received 19 December 2024, Revised 13 May 2025, Accepted 18 August 2025

ABSTRACT

This study provides a comprehensive guide for novice researchers to synthesize gold nanoparticles (AuNPs) with a target size of 15 nm using the Turkevich method. By employing a systematic approach, we successfully produced well-defined AuNPs with a moderate size distribution and spherical morphology. A step-by-step procedure flowchart of the synthesis procedure, along with equations for molar ratio calculations, is provided to assist novice researchers. A fixed molar ratio of 2.8 for the reducing agent to precursor was chosen, as previous studies indicate this ratio reliably yields nanoparticles of approximately 15 nm. Characterization techniques, including Ultra-High Resolution Scanning Electron Microscope (UHR-SEM), UV-visible spectroscopy, zeta potential measurements, and zeta sizer, were employed to confirm the desired properties. Additionally, Energy-Dispersive X-ray Spectroscopy (EDX) was utilized to verify the elemental composition of the nanoparticles, confirming the presence of pure gold and the absence of impurities. SEM analysis revealed an average particle size of 15 nm, aligning with the target size. Zeta potential measurements revealed an average value of -38.56 mV. Additionally, an average polydispersity index (PDI) of 0.367, obtained from triplicate measurements, further supports the monodisperse nature of the synthesized AuNPs. The synthesized AuNPs have potential applications in various fields, especially those requiring precisely sized particles, such as biomedicine and catalysis. Future research may focus on optimizing the synthesis process to enhance reproducibility and explore additional applications, including the production of AuNPs with different sizes by adjusting the molar ratio of reducing agent to precursors.

Keywords: *Gold nanomaterials; Turkevich method; nanoparticle synthesis; nanoparticle characterization; gold ion reduction*

1. INTRODUCTION

The Turkevich method, known for its simplicity and reproducibility, is a widely adopted chemical synthesis technique for producing spherical gold nanoparticles (AuNPs). The Turkevich method is favored by researchers due to its straightforward protocol using accessible reagents like gold chloride and sodium citrate. The method relies on the reduction of gold ions in solution, resulting in the formation of AuNPs [1]. Essential steps involve dissolving gold chloride ($AuCl_4$) in a solution, adding sodium citrate as a reducing agent, and initiating the reaction by heating the solution, resulting in the reduction of gold ions by citrate molecules and the formation of AuNPs [2]. The technique's versatility and mild reaction conditions make Turkevich-synthesized AuNPs broadly useful across diverse laboratories and fields, with prominent applications in areas like biomedicine, catalysis, electronics, and sensing, owing to the unique size-dependent optical, electronic, catalytic, and physiochemical properties of the nanoparticles. Researchers can optimize the Turkevich method to achieve specific properties in the synthesized nanoparticles by adjusting various parameters such as the molar ratio of the reagent mixture [3], [4], [5], [6], batch size [3], initial reagent concentration [3], temperature [3], [7], [8], [9], reaction time [10], pH [10], [11], the order of addition of the reagents [12], [13], [14] as well as the reducing and capping agent used [15]. Additionally, the addition of surfactants enhances the stability and dispersibility of nanoparticles in solution by attaching to their surface, lowering surface energy, limiting further growth, and confining them in the nanodomain [16]. Furthermore, it is worth highlighting that the utilization of flow reactors and pre-passivated precursors is yet another advantage of the Turkevich method. This method not only facilitates the production of gold nanoparticles but also enhances the reproducibility and control over the initial reaction stage. As a result, monodisperse nanoparticles with a narrow size distribution can be achieved consistently [17]. The optimization of the Turkevich method can lead to the synthesis of gold nanoparticles with specific properties tailored for various applications. Our study aimed to comprehensively explore the synthesis of gold nanoparticles (AuNPs) via the Turkevich method, focusing specifically on achieving a target size of 15 nm using a citrate-to-gold molar ratio of 2.8. While the Turkevich method for AuNP synthesis has been extensively studied and adapted across numerous works [4], [18], [19], [20], [21], [22], [23], [24], [25], [26], our approach specifically draws from Dong et al. [3], with modifications made to meet the objectives of this research. Building upon their foundational work, our experimental procedure focused exclusively on synthesizing 15 nm AuNPs, as the Turkevich method demonstrates reproducibility within the 10-30 nm range [27]. Additionally, this particular size is well-known

for its suitability in various applications due to its favourable physicochemical properties and stability [28], [29]. We employed the molar ratio of 2.8 (trisodium citrate dihydrate to gold(III) chloride), which Dong et al. identified as effective for producing particles of this size, with the expectation of achieving similar results. While maintaining the core parameter of a 2.8 molar ratio from Dong et al.'s work for synthesizing 15 nm AuNPs, our research addresses a common challenge in nanomaterial synthesis: the scarcity of detailed procedural information in published works, which often hinders result replication across different laboratories. Drawing upon our extensive literature review and experimental endeavours as newcomers, we encountered firsthand the frustration of piecing together critical details often omitted in reports of successful nanoparticle synthesis using the Turkevich method. To bridge this gap, the primary objective of this research is to provide a meticulously illustrated flowchart detailing the step-by-step synthesis procedure, an overview of molar ratio calculations, and transparent reporting of optimal synthesis parameters for well-defined, spherical 15 nm gold nanoparticles (AuNPs) using the traditional Turkevich method. The optimal synthesis parameters include precise volumes and concentrations of precursor and reducing agent, optimized reaction temperature profiles, as well as duration and speed for both stirring and centrifugation protocols.By explicitly detailing these parameters, we provide a tangible starting point for newcomers to fine-tune their own protocols. This approach transforms what is often an opaque and frustrating initiation for new researchers into a clear, data-rich roadmap, enabling them to rapidly establish synthesis protocols and progress to more advanced research questions. In short, our work not only aims to contribute to the growing body of knowledge on gold nanoparticle synthesis using the traditional Turkevich method but also addresses the common challenges faced by researchers new to this field. By providing comprehensive details on this well-established method, we offer a valuable resource for both novice and experienced researchers in the field of gold nanoparticle synthesis.

The characterization techniques, such as zeta potential measurement, zeta sizer, UHR-SEM, UV-Vis spectroscopy, and EDX, allow us to thoroughly investigate the physical, optical, and structural properties of the synthesized nanoparticles. UV-VIS spectroscopy gave insights into their optical properties, while zeta potential measurement with a zeta sizer provides a comprehensive evaluation of the colloidal system's stability and particle size distribution. This combination allows us to assess both the size of the particles as they exist in solution and the electrical forces that influence their stability and tendency to remain dispersed. UHR-SEM imaging revealed the surface morphology, agglomeration behavior, and precise size measurements of individual nanoparticles, providing a direct visual confirmation of the average particle size and size distribution. On the other hand, EDX confirmed the elemental composition of the nanoparticles, verifying their purity and composition. These analyses helped validate our approach in producing well-defined 15nm AuNPs using a specific molar ratio of 2.8. This research aspires to contribute valuable optimization knowledge, furthering understanding of the Turkevich method for the precise synthesis of 15nm AuNPs. Our findings hold critical implications for nanotechnology applications where the consistent and controlled production of specific nanoparticle sizes is pivotal.

2. MATERIALS AND METHODS

2.1. Materials

Gold (III) chloride solution (99.99% trace metals basis, 30 wt. % in dilute HCl) and trisodium citrate dehydrate (ACS reagent, ≥ 99.0%) were acquired from Sigma-Aldrich and Fisher Scientific, respectively. Deionized water served as the solvent for all experimental procedures.

2.2. Molar Ratio Overview: Experimental Approach in This Work for AuNP Synthesis

In gold nanoparticle (AuNP) synthesis, the molar ratio between reactants is a critical factor in controlling the properties of the final product, particularly size. This ratio, especially between the reducing agent and gold precursor, significantly influences the nucleation and growth processes of AuNPs.

A higher molar ratio of reducing agent to precursor translates to a greater number of reducing agent molecules available in the reaction mixture. This abundance of reducing agent molecules leads to faster reduction of the gold ions (Au^{3+}) to gold atoms (Au^{0}). Faster reduction allows for the formation of numerous nucleation sites, resulting in a larger number of smaller nanoparticles. Conversely, a lower molar ratio of reducing agent leads to slower reduction, favoring the growth of existing nuclei into fewer, larger nanoparticles.

Understanding and manipulating molar ratios allows researchers to tailor their syntheses for specific outcomes. The molar ratio is defined as the proportion of moles of two or more chemical species in a reaction, expressing the reaction's stoichiometry in terms of moles.

In this section, we provide a brief overview of the molar ratios we used in our experiments to synthesize gold nanoparticles with an expected size of 15 nm. We employed a sodium citrate to gold chloride molar ratio of 2.8.

Gold chloride ($HAuCl_4$) was obtained as a solution, and trisodium citrate dihydrate ($C_6H_9Na_3O_9$) as a powder. A mixture with a high molar concentration (34 mM) of trisodium citrate was prepared. A specific amount of trisodium citrate dihydrate powder was weighed and dissolved to create this concentrated solution. This solution was then used to precisely adjust the molar ratio to 2.8 with gold chloride, enabling controlled synthesis conditions that support reproducibility in similar experiments.

The calculation for the molar ratio of 2.8 for AuNP synthesis follows a systematic approach:

- First, the concentration and molar mass of $HAuCl_4$ and $C_6H_9Na_3O_9$, respectively, are provided by the manufacturer.
  - Concentration of $HAuCl_4$ solution is 1.45 mol/L
  - Molar mass of $C_6H_9Na_3O_9$ is 294.10 g/mol.

  Different parameters were considered for each reactant due to their original form (solution vs powder).
- Next, based on the desired molar ratios, the quantities of $HAuCl_4$ solution and $C_6H_9Na_3O_9$ powder required for each synthesis were calculated using the following methods:
  - To determine the amount of $HAuCl_4$ solution needed, we apply the dilution formula as represented by Eq. (1) :

$$C_i V_i = C_f V_f \quad (1)$$

In this equation, C_i and V_i are the initial concentration and volume of the solution, while C_f and V_f represent the final concentration and volume of the diluted solution, respectively. To prepare a 0.25 mM diluted solution in 50 mL of deionized water, we pipetted 8.62 µl from the stock solution.

  - To determine the amount of $C_6H_9Na_3O_9$ powder needed, we apply the formula as represented by Eq. (2) :

$$Mass\ weighed\ (g) = Concentration\ \left(\frac{mol}{L}\right) \times Volume\ (L) \times Molar\ mass\ of\ C_6H_9Na_3O_9\ \left(\frac{g}{mol}\right) \quad (2)$$

To prepare a 34 mM solution in 25 mL of deionized water, 0.25 g of $C_6H_9Na_3O_9$ powder was weighed from the stock.

- Following the determination of the required quantities of $HAuCl_4$ solution and $C_6H_9Na_3O_9$ powder, the number of moles for each reactant was calculated using Eq. (3).

$$Number\ of\ moles\ (mol) = Concentration\ \left(\frac{mol}{L}\right) \times Volume\ (L) \quad (3)$$

- The concentration and volume of $HAuCl_4$ are 0.25 mmol/L and 50.00862 mL, respectively.
- The concentration and volume of $C_6H_9Na_3O_9$ are 34 mmol/L and 1.03 mL, respectively.

- Finally, the molar ratio of 2.8 is calculated by dividing the number of moles of one reactant by the number of moles of the other reactant, as shown in Eq. (4).

$$Molar\ ratio\ (MR) = \frac{Number\ of\ moles\ C_6H_9Na_3O_9\ (mol)}{Number\ of\ moles\ HA_uCl_4\ (mol)} \quad (4)$$

Table 1. Preparation Details for Gold Nanoparticles at a Molar Ratio of 2.8

Trisodium Citrate Dihydrate		Gold (III) chloride		Final Molar Ratio Achieved
Mass of Trisodium Citrate Dihydrate Used (g) / Volume of Stock Solution Prepared (mL)	Volume of Trisodium Citrate Dihydrate Stock Solution Used (mL)	Concentration of Gold (III) Chloride Stock Solution (mM)	Volume of Gold (III) chloride pipetted from stock solution to dilute in 50 mL DI	
0.25 g in 25 mL DI	1.03	1.45	8.62 µL	2.8

Table 1 presents the parameters used to achieve the final molar ratio of 2.8 for the synthesis of gold nanoparticles. It includes the mass of trisodium citrate dihydrate used to prepare the concentrated stock solution, the volume of this stock solution utilized, the concentration of the gold (III) chloride stock solution, and the volume of gold (III) chloride pipetted for dilution. This table provides a detailed overview of the quantities and concentrations involved in the preparation process, offering clear reference points for replicating the experiment and understanding the specific conditions under which the final molar ratio was achieved. In our experiment, we used gold (III) chloride concentrations below 0.8 mM based on several key observations in the literature [3], [5], [30]. As introduced by Frens, Kimling et al.'s work established that while the gold-to-reductant ratio primarily determines particle size, the absolute concentration becomes crucial below 2 mM, with optimal size definition achieved at concentrations below 0.8 mM. At these lower concentrations, a narrow size dispersion of 13-16% can be attained for particles smaller than 40 nm [5]. They further reported a significant increase in both size and polydispersity when gold salt concentrations exceeded 0.8 mM, particularly at citrate-to-gold ratios below 2 [30]. This is further corroborated by

Zabetakis K. et al., who reported that lower initial $HAuCl_4$ concentrations (< 0.8 mM) result in reduced polydispersity [3].

2.3. Synthesis of AuNPs

All reaction vessels were meticulously cleaned prior to synthesis using acetone and deionized (DI) water. The vessels were then bath sonicated for 10 minutes with DI water. Figure 1 provides a comprehensive flowchart using text to detail the step-by-step procedures from initial preparation to completion. The entire synthesis process was carried out in a functional fume hood. In our procedures, 25 mL of 34.0 mM trisodium citrate dihydrate ($C_6H_9Na_3O_9$) solution was prepared by dissolving 0.25 gram in 25 mL DI water. After thorough stirring of the mixture, a 1.03 mL portion was carefully extracted using a syringe, and this sample was labelled as Sample A. Then, a 250 mL flask was used to prepare 50 mL of 0.25 mM gold chloride solution ($HAuCl_4$) separately. The solution was prepared by dissolving 8.62 µl of $HAuCl_4$ in 50 mL of DI water, namely Sample B. The $HAuCl_4$ solution (Sample B) was then heated on a hotplate while stirring at 1000 rpm. When the $HAuCl_4$ solution (sample B) attained a temperature of 90°C, sample A solution was promptly injected into it. The resulting mixture, namely sample C, underwent continuous heating and stirring for 5 minutes within the fume hood, during which a distinct color transition from light yellow to grey and ultimately to a wine red was observed. After the 5-minute duration, sample C was allowed to cool down naturally to room temperature. The cooled solution was then transferred to a centrifugation tube and subjected to centrifugation at 9000 rpm for 5 minutes.

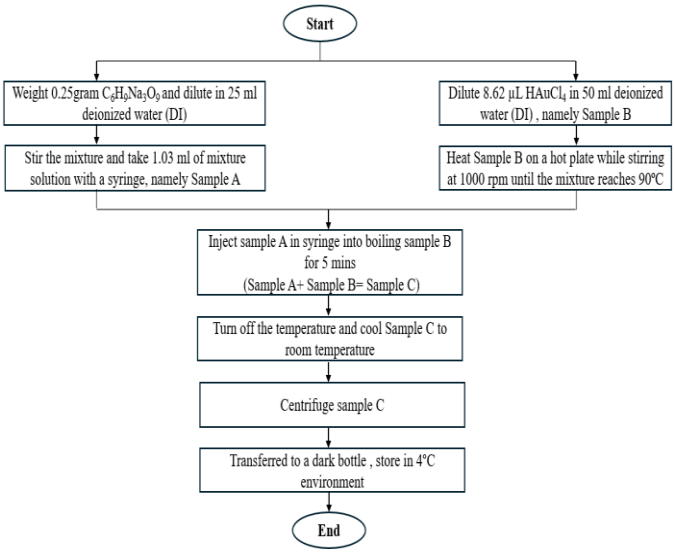

Figure 1. Turkevich AuNP synthesis flow at a 2.8 molar ratio

Figure 2 shows the separation of the cooled solution into a supernatant and a pellet after the centrifugation step. The supernatant, indicated by the clear liquid layer on top, contains the dispersed gold nanoparticles and other dissolved components. This supernatant fraction was carefully pipetted out and transferred to a dark bottle, where it was stored in a 4°C environment for further characterization analyses. The pellet, represented by the solid material at the bottom of the centrifuge tube, consisted of any denser particles, aggregates, or precipitates that sedimented during the centrifugation process. After separating the supernatant, the remaining pellet was diluted with deionized water before being discarded as waste.

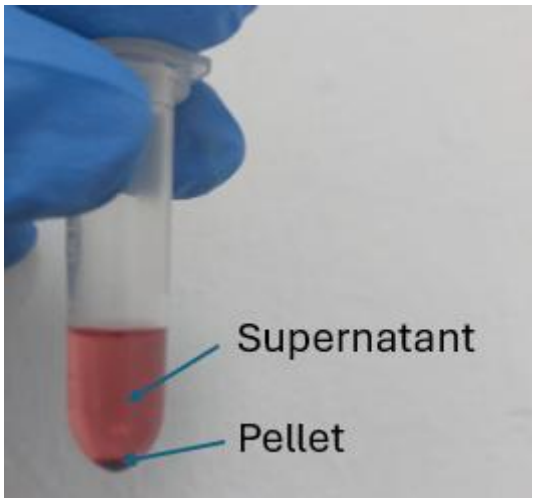

Figure 2. Separation of the synthesized gold nanoparticle solution after centrifugation

2.4. AuNP Sample Preparation: Solution-Based and Substrate Deposition Techniques

In this subsection, we describe the preparation and deposition methods of our synthesized AuNPs for various characterization techniques. Following the Turkevich synthesis method, the colloidal AuNP solution was used in both its original liquid form and as deposited films, depending on the specific analytical requirements. For UHR-SEM and EDX analyses, we employed the spin-coating technique. The spin-coating technique was performed using a two-step program, starting with a gradual increase in speed from 0 to 1000 rpm over 20 seconds, then maintaining a steady rotation at 1000 rpm for 90 seconds. In contrast, for zeta potential and zeta sizer measurements, as well as UV-Vis spectroscopy, we utilized the AuNPs in their original colloidal solution form. This approach preserves their native charge, size distribution, and optical properties, ensuring accurate assessment of their plasmonic characteristics and colloidal stability.

2.5. Characterization of AuNPs

The characterization of the synthesized AuNPs was carried out using a range of analytical techniques to comprehensively assess their properties. These techniques included spectroscopic methods for optical analysis, microscopy for morphological and elemental examination, and light scattering methods for determining particle size distribution and stability. Table 2 provides a summary of the instruments used in this study, detailing the specific

techniques, instrument types, brands, models, and the corresponding measurements obtained. This array of analytical tools allowed for a thorough investigation of the AuNPs' physicochemical properties, ensuring a robust characterization process.

Table 2. Analytical Instruments Used for AuNPs Characterization

Instrument	Brand	Model	Measurement
UHR-SEM	Hitachi	Regulus 8220	Size and shape of the nanoparticle
EDX Detector (integrated with UHR-SEM)	Oxford	Ultim Extreme	Elemental composition
UV-Vis Spectrophotometer	Perkin Elmer	Lamda 750	Optical properties
Zetasizer	Malvern	Master Sizer 2000	Zeta potential (mV)
Zetasizer	Malvern	Master Sizer 2000	Particle size distribution (PDI)

3. RESULT AND DISCUSSION

This section presents an examination of the synthesized gold nanoparticles' characteristics. Here, we focus on the comprehensive characterization of AuNPs using zeta potential measurement, zeta sizer, UHR-SEM, UV-Vis spectroscopy, and EDX. The tables, graphs, and figures in this section illustrate and support our findings, offering deeper insights into the morphological, optical, structural, and compositional properties of the AuNPs for the studied molar ratio.

3.1. Surface Morphology Observation

In this subsection, we present the UHR-SEM results, which offer direct visual confirmation of the nanoparticles' size and shape. These observations are pivotal for understanding the effectiveness of the synthesis conditions and verifying that the nanoparticles exhibit the intended characteristics. The images were captured at a consistent magnification of 80,000x, with observations made at two spots. The obtained images are presented in Figure 3.

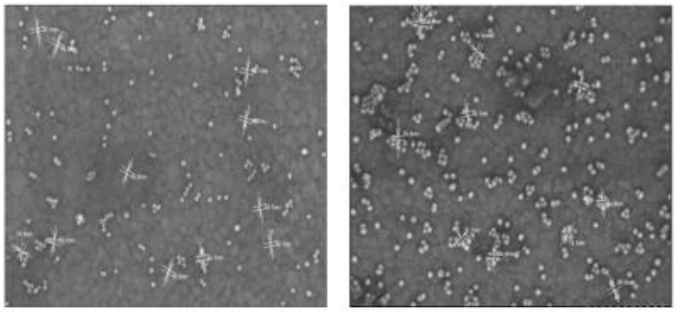

(a) (b)

Figure 3. UHR-SEM of AuNPs at (a) Spot 1, (b) Spot 2

Figure 3(a) and 3(b) present UHR-SEM micrographs of gold nanoparticles (AuNPs) synthesized using the Turkevich method, at two spots. The nanoparticles in these figures consistently exhibit sizes ranging from approximately 14.1 nm to 15.3 nm, which aligns with the hypothesis that a molar ratio of 2.8 produces AuNPs around 15 nm, as supported by previous literature. This consistency in size supports the hypothesis that the chosen synthesis conditions effectively produce AuNPs of the desired size. UHR-SEM imaging also confirmed the spherical shape of these nanoparticles, further demonstrating the effectiveness of the synthesis conditions in achieving uniform morphology. In each figure, the nanoparticles exhibit a predominantly spherical morphology, which is advantageous for applications requiring uniform particle shape and surface properties. This spherical shape indicates successful control over the synthesis process, as intended. Some degree of agglomeration is visible in all figures, with nanoparticles clustering into larger aggregates. Despite this, the individual nanoparticles remain spherical in shape. The zeta potential results indicate moderate stability, allowing the observed agglomeration to be disregarded. In summary, these figures collectively demonstrate the successful synthesis of spherical AuNPs with the desired size around 15 nm and spherical morphology.

3.2. Stability and Particle Size Distribution

These analyses complement our previous findings on size and shape, providing crucial information about the nanoparticles' surface charge, stability, and size distribution uniformity. The zeta potential, reported in millivolts (mV), offers insights into the electrostatic stabilization of the AuNPs in solution. Concurrently, the PDI, determined using Zeta sizer, quantifies the homogeneity of the nanoparticle population. The findings of our work, summarized in Table 3, demonstrate that utilizing a 2.8 molar ratio yields AuNPs with satisfactory colloidal stability and acceptable size distribution uniformity.

Table 3. Characteristics of Gold Nanoparticles Synthesized Using a Molar Ratio of 2.8

Parameter	Value
Monodispersity (PDI)	0.367
Stability	-38.56 mV

The data presented in Table 3 reveal several important characteristics of the gold nanoparticles (AuNPs) synthesized using the chosen citrate-to-gold ratio of 2.8.

Polydispersity Index (PDI) is a key parameter that represents the distribution of size populations within a given nanoparticle sample. The numerical value of PDI ranges from 0.0 to 1.0, where 0.0 indicates a perfectly uniform sample with respect to particle size, and 1.0 represents a highly polydisperse sample with multiple particle size populations [31]. The moderate polydispersity

index (PDI) of 0.367 obtained in this work, which is an average value obtained from three separate Zeta Sizer measurements of the same sample, reflects a relatively moderate size distribution with some variability in particle size. This average PDI indicates that, while there is some size variation among the nanoparticles, the overall distribution is reasonably controlled.

Zeta potential (ZP) is a crucial parameter that provides valuable insights into the stability of nano dispersions. Generally, higher absolute values of zeta potential suggest a greater probability of suspension stability. Colloidal systems with absolute ZP values in the range of 31 to 40 mV are often considered to have moderate stability. Conversely, small ZP values (from +5 to −5 mV) typically indicate a tendency for system destabilization [32]. In these cases (low potentials), attractive forces may exceed repulsive forces, potentially leading to coagulation or flocculation [2][33][34]. In our case, the notably negative ZP of -38.56 mV, which is an average value derived from three separate measurements, indicates strong electrostatic repulsion between particles. This high negative value suggests that the citrate ions provide effective stabilization, minimizing particle aggregation and enhancing the stability of the colloidal dispersion.

The use of multiple measurements from the same sample for both polydispersity index (PDI) and zeta potential (ZP) ensures that the average values accurately represent the size distribution and stability characteristics within that specific sample.

3.3. Optical Properties and Localized Surface Plasmon Resonance (LSPR) Behavior

In our investigation of AuNP synthesis via the Turkevich method, UV-Vis spectroscopy provided crucial insights into the relationship between citrate-to-gold ratio and nanoparticle characteristics. The observed spectral shifts and peak characteristics correlated strongly with particle size, dispersity, and morphology as confirmed by complementary techniques.

The band intensity and wavelength in UV-Vis spectra depend on various AuNP properties, including structure, shape, metal composition, and size [35], [36], [37]. Typically, spherical AuNPs of approximately 10 nm diameter exhibit a surface plasmon band with peaks around 521 nm [2]. As particle size increases, the wavelength of this peak shift to higher values [37]. This relationship between particle size and spectral characteristics formed the basis for interpreting our results.

Figure 4 presents the UV-Vis spectrum of our gold nanoparticle sample, synthesized using the Turkevich method. A prominent, single peak is centered at 521 nm. Interestingly, this wavelength is typically reported for 10 nm AuNPs [2], but our nanoparticles, with an average size of approximately 15 nm, exhibit the same SPR peak position.

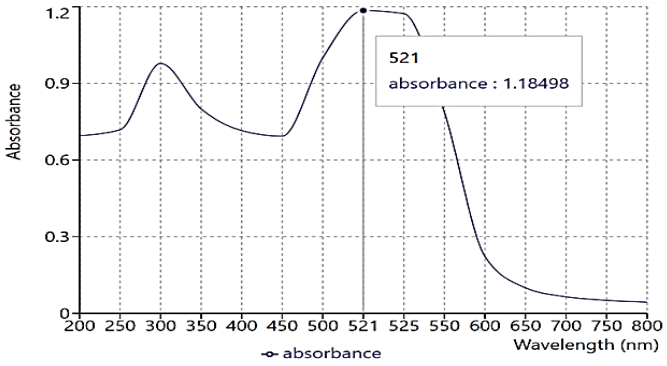

Figure 4. UV-Vis spectrum of synthesized gold nanoparticles using MR of 2.8

While the literature suggests that larger nanoparticles generally show a red-shift in the SPR peak [2], the observed result can be explained by several factors. Gold nanoparticles with a spherical shape tend to have more predictable SPR behavior compared to non-spherical particles, which often show more significant peak shifts as their size changes. In our case, the spherical shape of the nanoparticles likely contributes to the stability of the SPR peak, limiting the wavelength shift even with the size increase to 15 nm. Additionally, the moderately broad peak and the polydispersity index (PDI) of 0.367 from our zeta sizer analysis suggest a moderate size distribution, with some smaller particles likely contributing to the optical response. The spherical shape and relatively narrow size range (14.1–15.3 nm), confirmed by UHR-SEM analysis, further support the idea that the expected red-shift in the SPR peak is minimized despite the increase in particle size. In conclusion, while our AuNPs have a larger average size than 10 nm, the observed SPR peak at 521 nm is consistent with the combined effects of particle size distribution and shape. This demonstrates successful synthesis with controlled growth and a moderately uniform size distribution, corroborated by UHR-SEM and zeta sizer results.

3.4. Elemental Composition Assessment

To further assess the elemental composition and purity of the synthesized gold nanoparticles, energy-dispersive X-ray spectroscopy (EDX) analysis was performed. Our EDX results reveal a significant composition of gold, along with other elements such as carbon, oxygen, chloride, and sodium. These findings provide a comprehensive understanding of the elemental makeup of the nanoparticles, confirming the successful synthesis and highlighting the presence of residual components from the synthesis process. The results of the EDX analysis are summarized in Table 4.

Table 4 presents a detailed summary of the elemental composition data obtained from EDX analysis. The EDX analysis of the gold nanoparticles synthesized using the Turkevich method, where trisodium citrate dihydrate was employed as the reducing agent and gold (III) chloride as

the precursor, reveals a significant composition of 25.75% gold, indicating successful synthesis of gold nanoparticles. The detection of carbon in the EDX analysis corroborates the presence of the citrate capping layer on the AuNPs.

Table 4. Elemental Composition of Synthesized Gold Nanoparticles using MR of 2.8

Element	Weight% (EDX)
Gold (Au)	25.75
Oxygen (O)	1.70
Carbon (C)	64.59
Chloride (Cl)	6.89
Sodium (Na)	1.07

The high carbon content (64.59%) is due to the citrate ions from the reducing agent, which remain on the nanoparticle surface. The high percentage of carbon and gold suggests a gold-coated carbon-based material. Chloride (6.89%) and sodium (1.07%) are likely remnants from the gold (III) chloride precursor and the trisodium citrate, respectively. This elemental composition confirms the successful reduction of gold ions and formation of gold nanoparticles, with some residual components from the synthesis process. Additionally, the presence of oxygen (1.70%) can be attributed to the citrate capping agent used during synthesis. Hence, our results confirm the reliability of our transparent approach, effectively aiding novice researchers in understanding the relationship between synthesis parameters and nanoparticle characteristics.

4. CONCLUSION

In this study, we successfully synthesized gold nanoparticles (AuNPs) using the Turkevich method with a suggested molar ratio of reducing agent to precursor (2.8). This approach achieved a target size of 15 nm, demonstrating a reliable and reproducible method for novice researchers. The consistent reaction conditions and systematic methodology resulted in well-defined AuNPs with a moderate size distribution and spherical morphology. Comprehensive characterization confirmed the desired properties, including an average particle size of 15 nm with strong electrostatic repulsion preventing aggregation. The EDX analysis reveals an acceptable gold content, coupled with the detection of the citrate capping agent, which indicates the synthesis of AuNPs with the desired surface functionality. The inclusion of detailed molar ratio calculations in our work provides a valuable resource for novice researchers, offering guidance on how to modify the synthesis process to achieve their desired nanoparticle size. While our protocol reliably produces 15 nm AuNPs, the optimization of parameters such as reagent concentration, temperature, pH, and reaction time remains necessary for controlling particle characteristics such as their size, shape, dispersity, and stability. Future research should explore tuning these variables, alongside molar ratio adjustments, to enhance reproducibility and achieve application-specific outcomes.

ACKNOWLEDGMENTS

This research was made possible through the generous support of various institutions, including Universiti Teknologi MARA (UiTM), the Ministry of Higher Education (MOHE), and the Institut Pengajian Siswazah (IPSis). Specifically, UiTM provided essential facilities, while MOHE provided funding under the Fundamental Research Grant Scheme (FRGS) (FRGS/1/2023/TK07/UITM/02/26) to facilitate the purchase of materials required for the study as well as the rental of advanced equipment for characterization and analysis. Additionally, IPSis contributed funding for the journal publication fees.

REFERENCES

[1] S. S. Priyadarshini, "Innovative and sustainable approaches to gold nanoparticle synthesis: beyond the Turkevich method," *Journal of Nanomaterials and Devices*, vol. 1, no. 1, pp. 1–5, 2023, doi: 10.61577/jnd.2023.100004.

[2] A. E. F. Oliveira, A. C. Pereira, M. A. C. Resende, and L. F. Ferreira, "Gold Nanoparticles: A Didactic Step-by-Step of the Synthesis Using the Turkevich Method, Mechanisms, and Characterizations," *Analytica*, vol. 4, no. 2, pp. 250–263, Jun. 2023, doi: 10.3390/analytica4020020.

[3] J. Dong, P. L. Carpinone, G. Pyrgiotakis, P. Demokritou, and B. M. Moudgil, "Synthesis of precision gold nanoparticles using Turkevich method," *KONA Powder and Particle Journal*, vol. 37, pp. 224–232, 2020, doi: 10.14356/kona.2020011.

[4] Z. Bahmanyar, F. Mohammadi, A. Gholami, and M. Khoshneviszadeh, "Effect of different physical factors on the synthesis of spherical gold nanoparticles towards cost-effective biomedical applications," *IET Nanobiotechnol*, vol. 17, no. 1, pp. 1–12, Feb. 2023, doi: 10.1049/nbt2.12100.

[5] J. Kimling, M. Maier, B. Okenve, V. Kotaidis, H. Ballot, and A. Plech, "Turkevich method for gold nanoparticle synthesis revisited," *Journal of Physical Chemistry B*, vol. 110, no. 32, pp. 15700–15707, Aug. 2006, doi: 10.1021/jp061667w.

[6] N. E. Larm et al., "Room-Temperature Turkevich Method: Formation of Gold Nanoparticles at the Speed of Mixing Using Cyclic Oxocarbon Reducing Agents," *The Journal of Physical Chemistry C*, vol. 122, no. 9, pp. 5105–5118, Mar. 2018, doi: 10.1021/acs.jpcc.7b10536.

[7] P. Dobrowolska, A. Krajewska, M. Gajda-Raczka, B. Bartosewicz, P. Nyga, and B. J. Jankiewicz, "Application of turkevich method for gold nanoparticles synthesis to fabrication of SiO_2@Au and TiO_2@Au core-shell nanostructures," *Materials*, vol. 8, no. 6, pp. 2849–2862, 2015, doi: 10.3390/ma8062849.

[8] A. H. Bari, N. Shukla, A. Gavriilidis, and A. A. Kulkarni, "Transient response to perturbations in flow synthesis of citrate capped gold nanoparticles," *Chemical Engineering Journal*, vol. 470, p. 143890, Aug. 2023, doi: 10.1016/j.cej.2023.143890.

[9] N. Gul et al., "Size controlled synthesis of silver nanoparticles: A comparison of modified Turkevich and BRUST methods," *Zeitschrift für Physikalische Chemie*, vol. 236, no. 9, pp. 1173–1189, 2022, doi: 10.1515/zpch-2022-0009.

[10] S. Yazdani et al., "Model for Gold Nanoparticle Synthesis: Effect of pH and Reaction Time," *ACS Omega*, vol. 6, no. 26, pp. 16847–16853, Jul. 2021, doi: 10.1021/acsomega.1c01418.

[11] H. Tyagi, A. Kushwaha, A. Kumar, and M. Aslam, "A Facile pH Controlled Citrate-Based Reduction Method for Gold Nanoparticle Synthesis at Room Temperature," *Nanoscale Research Letters*, vol. 11, no. 1, p. 362, Dec. 2016, doi: 10.1186/s11671-016-1576-5.

[12] Z. B. Afrapoli, R. F. Majidi, B. Negahdari, and G. Tavoosidana, "'Inversed Turkevich' method for tuning the size of Gold nanoparticles: Evaluation the effect of concentration and temperature," *Nanomedicine Research Journal*, vol. 3, no. 4, pp. 190–196, 2018, doi: 10.22034/NMRJ.2018.04.003.

[13] I. Ojea-Jiménez, N. G. Bastús, and V. Puntes, "Influence of the sequence of the reagents addition in the citrate-mediated synthesis of gold nanoparticles," *The Journal of Physical Chemistry C*, vol. 115, no. 32, pp. 15752–15757, Aug. 2011, doi: 10.1021/jp2017242.

[14] S. K. Sivaraman, S. Kumar, and V. Santhanam, "Monodisperse sub-10 nm gold nanoparticles by reversing the order of addition in Turkevich method – The role of chloroauric acid," *Journal of Colloid and Interface Science*, vol. 361, no. 2, pp. 543–547, Sep. 2011, doi: 10.1016/j.jcis.2011.06.015.

[15] A. M. Figat et al., "α-Amino Acids as Reducing and Capping Agents in Gold Nanoparticles Synthesis Using the Turkevich Method," *Langmuir*, vol. 39, no. 25, pp. 8646–8657, Jun. 2023, doi: 10.1021/acs.langmuir.3c00507.

[16] J. Najeeb et al., "Surfactant stabilized gold nanomaterials for environmental sensing applications – A review," *Environmental Research*, vol. 208, May 2022, doi: 10.1016/j.envres.2021.112644.

[17] L. Panariello et al., "Highly reproducible, high-yield flow synthesis of gold nanoparticles based on a rational reactor design exploiting the reduction of passivated Au(III)," *Reaction Chemistry & Engineering*, vol. 5, no. 4, pp. 663–676, Apr. 2020, doi: 10.1039/c9re00469f.

[18] M. Matamoros-Ambrocio et al., "A comparative study of gold impregnation methods for obtaining metal/semiconductor nanophotocatalysts: Direct turkevich, inverse turkevich, and progressive heating methods," *Catalysts*, vol. 8, no. 4, p. 161, Apr. 2018, doi: 10.3390/catal8040161.

[19] M. Wuithschick et al., "Turkevich in New Robes: Key Questions Answered for the Most Common Gold Nanoparticle Synthesis," *ACS Nano*, vol. 9, no. 7, pp. 7052–7071, Jul. 2015, doi: 10.1021/acsnano.5b01579.

[20] L. Shi, E. Buhler, F. Boué, and F. Carn, "How does the size of gold nanoparticles depend on citrate to gold ratio in Turkevich synthesis? Final answer to a debated question," *Journal of Colloid and Interface Science*, vol. 492, pp. 191–198, Apr. 2017, doi: 10.1016/j.jcis.2016.10.065.

[21] B. Bartosewicz et al., "Effect of citrate substitution by various α-hydroxycarboxylate anions on properties of gold nanoparticles synthesized by Turkevich method," *Colloids and Surfaces A: Physicochemical and Engineering Aspects*, vol. 549, pp. 25–33, Jul. 2018, doi: 10.1016/j.colsurfa.2018.03.073.

[22] K. Sreejivungsa and P. Thongbai, "Enhanced dielectric properties of PVDF polymer nanocomposites: A study on gold-decorated, surface-modified multiwalled carbon nanotubes," *Heliyon*, vol. 10, no. 4, Feb. 2024, doi: 10.1016/j.heliyon.2024.e26693.

[23] Y. O. Ibrahim et al., "Gold nanoparticles spectral CT imaging and limit of detectability in a new materials contrast-detail phantom," *Physica Medica*, vol. 120, Apr. 2024, doi: 10.1016/j.ejmp.2024.103326.

[24] P. Ann Rose et al., "Studies on thermal diffusion of aqueous solution of zinc oxide (ZnO) microtubes in gold (Au) using dual beam thermal lens experiment," *Materials Today: Proceedings*, Elsevier Ltd, 2023, pp. 1099–1102, doi: 10.1016/j.matpr.2023.05.135.

[25] Y. Zhang et al., "Sub-100 fs Yb:CALGO laser based on gold nanoparticles saturable absorber," *Optik*, vol. 288, Oct. 2023, doi: 10.1016/j.ijleo.2023.171169.

[26] V. P. Ozcan et al., "The effect of the gold nanoparticles and gold nano-clusters on the behavior of natural lung surfactant," *Journal of Molecular Liquids*, vol. 387, Oct. 2023, doi: 10.1016/j.molliq.2023.122616.

[27] T. M. S. Erlangga, A. B. D. Nandiyanto, and R. Ragadhita, "Preliminary reactor design for the gold nanoparticles production by the Turkevich method on an industrial scale," *Sustainable Engineering and Innovation*, vol. 5, no. 1, pp. 22–30, Feb. 2023, doi: 10.37868/sei.v5i1.id191.

[28] X. Y. Liu et al., "A simply visual and rapidly colorimetric detection of Hg^{2+} in cosmetics based on gold nanoparticles modified by sulfadiazine," *Optical Materials*, vol. 137, Mar. 2023, doi: 10.1016/j.optmat.2023.113622.

[29] E. Engels et al., "Efficacy of 15 nm Gold Nanoparticles for Image-Guided Gliosarcoma Radiotherapy," *Journal of Nanotheranostics*, vol. 4, no. 4, pp. 480–495, Oct. 2023, doi: 10.3390/jnt4040021.

[30] K. Zabetakis et al., "Effect of high gold salt concentrations on the size and polydispersity of gold nanoparticles prepared by an extended Turkevich–Frens method," *Gold Bulletin*, vol. 45, no. 4, pp. 203–211, Dec. 2012, doi: 10.1007/s13404-012-0069-2.

[31] M. Danaei et al., "Impact of particle size and polydispersity index on the clinical applications of

lipidic nanocarrier systems," *Pharmaceutics*, May 2018, doi: 10.3390/pharmaceutics10020057.

[32] I. Ostolska and M. Wiśniewska, "Application of the zeta potential measurements to explanation of colloidal Cr_2O_3 stability mechanism in the presence of the ionic polyamino acids," *Colloid and Polymer Science*, vol. 292, no. 10, pp. 2453–2464, Oct. 2014, doi: 10.1007/s00396-014-3276-y.

[33] S. Banerjee et al., "A regular rippled pattern formed by the molecular self-organization of polyvinylpyrrolidone encapsulated Ag nanoparticles: a high transmissive coating for efficiency enhancement of c-Si solar cells," *RSC Advances*, vol. 5, no. 8, pp. 5667–5673, 2015.

[34] G. W. Lu and P. Gao, "Emulsions and Microemulsions for Topical and Transdermal Drug Delivery," in *Handbook of Non-Invasive Drug Delivery Systems*, William Andrew, 2010, pp. 59–94, doi: 10.1016/B978-0-8155-2025-2.10003-4.

[35] J. Jana, M. Ganguly, and T. Pal, "Enlightening surface plasmon resonance effect of metal nanoparticles for practical spectroscopic application," *RSC Advances*, vol. 6, no. 89, pp. 86174–86211, 2016, doi: 10.1039/C6RA14173K.

[36] D. Sevenler, N. L. Ünlü, and M. S. Ünlü, "Nanoparticle biosensing with interferometric reflectance imaging," in *Nanobiosensors and Nanobioanalyses*, Springer Japan, 2015, pp. 81–95, doi: 10.1007/978-4-431-55190-4_5.

[37] K. G. Thomas, "Surface Plasmon Resonances in Nanostructured Materials," in *Nanomaterials Chemistry*, Wiley, 2007, pp. 185–218, doi: 10.1002/9783527611362.ch6.